

LASER APPLICATIONS AND OTHER TOPICS IN QUANTUM ELECTRONICS https://doi.org/10.1070/QEL16493

Development of a laser system of the laboratory AVLIS complex for producing isotopes and radionuclides

A.B. D'yachkov, A.A. Gorkunov, A.V. Labozin, S.M. Mironov, V.Ya. Panchenko, V.A. Firsov, G.O. Tsvetkov

Abstract. **The use of atomic vapour laser isotope separation (AVLIS) for solving a number of urgent problems (formation of ^{177}Lu radionuclides for medical applications, ^{63}Ni radionuclides for betavoltaic power supplies and ^{150}Nd isotope for searching for neutrinoless double β decay and neutrino mass) is considered. An efficient three-step scheme of photoionisation of neodymium atoms through the 50474-cm^{-1} autoionising state with radiation wavelengths of the corresponding stages of λ_1 = 6289.7 Å, λ_2 = 5609.4 Å and λ_3 = 5972.1 Å is developed. The average saturation intensity of the autoionising transition is $\sim$6 W cm^{-2}, a value consistent with the characteristics of the previously developed photoionisation schemes for lutetium and nickel. A compact laser system for the technological AVLIS complex, designed to produce radionuclides and isotopes under laboratory conditions, is developed based on the experimental results.**

Keywords: *laser isotope separation, copper vapour laser, dye laser, autoionising state.*

1. Introduction

Recent technological progress in the production of isotopes and radionuclides put forward a number of problems, such as the production of ^{177}Lu radioisotopes for medical applications and ^{63}Ni radioisotopes for betavoltaic autonomous power supplies, as well as the selection of ^{150}Nd isotope from a natural mixture (the natural content of ^{150}Nd is 5.6%) to search for the double neutrinoless β decay and neutrino mass. A promising (from the point of view of lowering cost and enhancing safety) technology for solving the aforementioned problems is the technique of atomic vapour laser isotope separation (AVLIS) [1, 2]. One of the factors limiting the development of this method is the high cost of laser radiation. Therefore, the efficiency of its application is of key importance.

The essence of the AVLIS method is the selective laser photoionisation of target isotope atoms with subsequent selection of newly formed photoions from an atomic flux using electrostatic fields. The ability of laser radiation to form photoions is determined by the photoionisation cross section σ:

A.B. D'yachkov, A.A. Gorkunov, A.V. Labozin, S.M. Mironov, V.Ya. Panchenko, V.A. Firsov, G.O. Tsvetkov National Research Center 'Kurchatov Institute', pl. Akad. Kurchatova 1, 123182 Moscow, Russia; e-mail: glebtsvetkov@mail.ru

Received 11 August 2017; revision received 6 October 2017
Kvantovaya Elektronika **48** (1) 75–81 (2018)
Translated by Yu.P. Sin'kov

$$\frac{dN_i}{dt} = N_a \sigma I, \quad (1)$$

where N_i and N_a are, respectively, the numbers of photoions and atoms on the propagation path of a laser beam with a cross-sectional area of 1 cm^2, and I (in cm^{-2} s^{-1}) is the fluence of laser photons. Assuming (in the first approximation) that photoionisation occurs with a constant rate during a pulse of width τ (in seconds), one can find that the number of photoions by the end of the pulse is

$$N_i \approx N_a \sigma I \tau. \quad (2)$$

An efficient use of an evaporated material implies that the number of photoions constitutes a significant fraction of the number of atoms, i.e.,

$$I \approx 1/(\sigma\tau). \quad (3)$$

Concerning the efficiency of applying laser radiation, an important factor is the fraction of laser radiation used for photoionisation. This fraction, given by the expression

$$N_i/(I\tau) \approx N_a \sigma \quad (4)$$

depends, along with the cross section, on the number of atoms on the laser beam propagation path. If this number is small, only a small part of laser radiation is spent. The efficiency of laser beam application can be enhanced by increasing the number of atoms, as a result of which the radiation absorption coefficient increases and some atoms fall under conditions of low photon fluence; as a result, conditions (3) are violated. An arbitrary compromise is an observable but rather small absorption coefficient, e.g., 0.1:

$$N_a \sigma \approx 0.1. \quad (5)$$

The number of atoms on the laser beam propagation path can be written as a product of the concentration n of target isotope atoms and the evaporator length L. Then one has

$$L \approx 0.1/(n\sigma). \quad (6)$$

It follows from formulas (3) and (6) that the scale of the system (laser power and evaporator length) and, correspondingly, its cost increase with decreasing photoionisation cross section σ. For example, in the photoionisation schemes of lutetium [3] and nickel [4], the photoionisation cross sections are $\sim 10^{-15}$ cm^2; thus, a laboratory setup with an average power of a laser system of several watts and evaporator length

of ~1 m turns out to be quite efficient when using the laser system conventional for AVLIS: a dye laser (DL) pumped by a copper vapour laser (CVL). However, in the scheme of neodymium photoionisation [5] (the photoionisation cross section is $\sim 10^{-17}$ cm^2), the desired efficiency is obtained only in a commercial system with an average power of several hundred watts and an evaporator length of several tens of meters. This is consistent well with the problem of producing several hundred kilograms of enriched neodymium, an amount necessary for searching for the neutrino mass [6]. The development of such a large system is highly expensive, which is a hindrance for implementing the AVLIS method. It should be noted that specifically high risks of implementing the new technology led to curtailing the programme of incorporating the AVLIS into the production of enriched uranium in the United States at the turn of the 20th and 21st centuries [7].

The risks related to the implementation of AVLIS technology can be significantly reduced by developing it step by step, starting with an efficient laboratory setup. To use efficiently laser radiation and evaporated material under laboratory conditions, one needs a new scheme of neodymium photoionisation with a photoionisation cross section of $\sim 10^{-15}$ cm^2. This scheme will make it possible to develop a unified technological laser complex for producing ^{177}Lu and ^{63}Ni radionuclides, as well as ^{150}Nd isotope.

2. Development of the photoionisation scheme of neodymium atoms

The experience in searching for three-step photoionisation schemes [5] shows that the spectrum of Nd I does not contain any odd autoionising states with large photoionisation cross sections, except for the level with an energy $E = 50474$ cm^{-1} [8]. However, the three-step scheme involving this state, which was proposed in [8], is characterised by a small isotopic frequency shift in the first transition, as a result of which one cannot obtain sufficiently high selectivity [5]. Therefore, a new photoionisation scheme must be sought for; this search was performed in two directions.

The first way is to search for an autoionising state with a high photoionisation cross section among even states. Neodymium atoms can be excited (using two dipole transitions) from the even ground state to an even autoionising state with an energy exceeding the ionisation threshold: 44562 cm^{-1}. The frequency of one of these transitions must lie in the UV spectral range, and the frequency of the other must be in the visible range.

The second way is to use the high cross section of photoionisation through the known level with an energy of 50474 cm^{-1}. To implement this possibility, it was necessary to find a combination of transitions that, on the one hand, would be characterised by a significant isotopic frequency shift (~1 GHz) and provide high selectivity and, on the other hand, would make it possible to excite neodymium atoms to the autoionising state with an energy of 50474 cm^{-1}.

The energy level diagram of neodymium is one of the most complicated among the energy level diagrams of lanthanides. This complexity is explained by the partial filling of the *f* shell, which contains four electrons in the ground state, whose energies are close to those of *d* electrons. Despite the large amount of data on the energy levels of Nd I [9, 10], the neodymium spectrum remains hardly studied, with a large number of unclassified levels and transitions. Especially scarce are the data on the high-lying states with energies above 31000 cm^{-1}. The last (found by us) spectroscopic data on Nd I were published almost 15 years ago [11, 12].

When developing a two-step scheme of excitation to an even autoionising state, one must take into account that UV laser radiation is obtained by frequency doubling in a nonlinear crystal, as a result of which the radiation power is significantly limited. In this context, we restricted ourselves to the consideration of schemes based on an UV transition from the ground state, because the absorption cross sections for the first transitions are generally much larger than the ionisation cross sections. In addition, the results of studying the isotopic shift [13] suggest that these transitions may include those characterised by large isotopic frequency shifts.

Table 1 contains the line parameters for the strongest transitions from the ground Nd I state, which were found by us in the wavelength range of 3028–3233 Å, and the isotopic shifts between the transition frequencies in ^{142}Nd and ^{144}Nd. For the transitions having the largest isotopic shifts, the shifts between the transition frequencies in ^{148}Nd and ^{150}Nd were also measured. Despite the fact that the magnitude of the isotopic frequency shift for the transitions found in the UV region exceeds that for the transition with $\lambda_1 = 5967.64$ Å in the photoionisation scheme [5], one should not expect the photoionisation selectivity to increase, because the ratio of the isotopic shifts to the Doppler widths for these transitions is much smaller.

Table 1. Isotopic frequency shifts $\Delta\nu_{142-144}$ and $\Delta\nu_{148-150}$ of the strongest transitions from the Nd I ground state, found in the wavelength range of 3028–3223 Å; the ratios of the isotopic shifts to Doppler linewidths at a neodymium evaporation temperature of 1900 K; and similar characteristics of the three transitions in the visible spectral range (the measurement error $\Delta\nu$ is ±30 MHz).

Transition line wavelength in vacuum/Å	Transition energy/cm^{-1}	Isotopic frequency shift of transition, $\Delta\nu_{142-144}$ ($\Delta\nu_{148-150}$) /GHz	Ratio of $\lvert\Delta\nu_{148-150}\rvert$ to the Doppler linewidth
3027.736	33027.98	–1.40 (–1.75)	0.69
3073.764	32533.40	–1.26 (–1.57)	0.63
3087.192	32391.90	–1.04	–
3094.786	32312.42	–0.95	–
3188.381	31363.88	–1.03 (–1.39)	0.58
3191.617	31332.09	–0.55	–
3191.992	31328.40	–0.94	–
3194.169	31307.04	–0.26	–
3195.333	31295.64	–0.34	–
3208.585	31166.39	–0.57	–
3214.209	31111.86	–0.90	–
3217.835	31076.80	–0.86	–
3223.330	31023.81	–1.11 (–1.30)	0.55
5889.506	16979.352	–0.224 (–0.106) [14]	0.08
5967.641	16757.039	–0.872 (–1.127) [14]	0.88
6289.743	15898.902	–0.674 (–0.802) [14]	0.66

For the transition with $\lambda_1 = 3027.736$ Å, which is characterised by the largest measured isotopic shift, we sought for transitions to the autoionising states with energies $E = 49667 - 50573$ cm^{-1}. The characteristics of the found transitions are listed in Table 2.

In the photoionisation scheme with $\lambda_1 = 3027.736$ Å and $\lambda_2 = 5929.843$ Å, we investigated the dependences of the photoion current on the average laser beam intensity at the first- and second-transition frequencies (Figs. 1, 2). It can be seen

Table 2. Energies of even autoionising levels of Nd I, wavelengths (in vacuum) of the lines of the corresponding autoionising transitions in ^{142}Nd from the level with energy of 33027.984 cm^{-1}, and the ratios K of the photoionisation current through an autoionising state to the photoionisation current in continuum at an average laser beam intensity of 2.5 W cm^{-2}.

Wavelength of autoionising transition line/Å	Energy of autoionising state/cm^{-1}	K
6004.21	49682.96	4
5981.70	49745.65	4
5964.91	49792.69	10
5964.16	49794.81	6
5953.07	49826.03	2
5952.47	49827.73	3
5946.61	49844.30	4
5930.42	49890.20	7
5929.84	49891.84	12
5929.29	49893.40	14
5908.40	49953.03	5
5871.79	50058.57	4
5765.57	50372.32	4

that the saturation of transition to an autoionising state calls for laser radiation with an average intensity of 80 W cm^{-2}, which corresponds to a photoionisation cross section less than 10^{-16} cm^2. The results show that, although no photoionisation scheme with a large cross section was found in the first stage, the search among two-step schemes should be considered as promising. The work in this field will be continued.

The second direction of search is related to the development of a three-step photoionisation scheme through the autoionising state having an energy of 50474 cm^{-1}; this state was found by Zyuzikov et al. [8], who proposed a photoionisation scheme with λ_1 = 5889.51 Å and $\lambda_2 = \lambda_3$ = 5971 Å, involving the aforementioned autoionising level (Fig. 3). The isotopic shifts between the frequencies of transitions with λ_1 = 5889.51 Å in ^{148}Nd and ^{150}Nd is only –0.11 GHz [14] (Table 1); hence, this scheme cannot be applied directly to select efficiently the ^{150}Nd isotope from a natural mixture. It is noteworthy that the total electron momentum J of the first excited level with

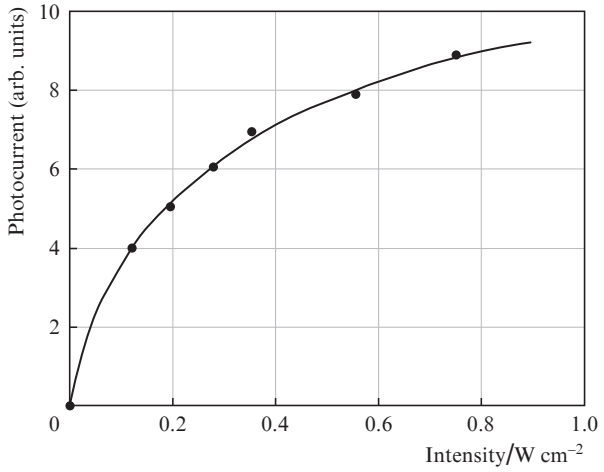

Figure 1. Dependence of the photoion current on the average excitation radiation intensity (λ_1 = 3027.736 Å) at an ionising radiation intensity of 3 W cm^{-2}.

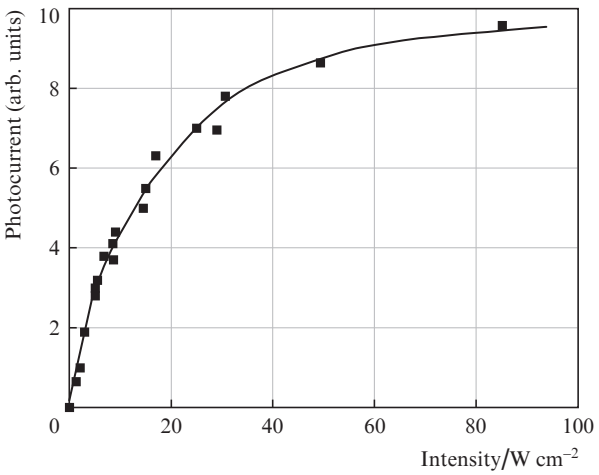

Figure 2. Dependence of the photoion current on the average ionising radiation intensity (λ_2 =5929.843 Å) at an average excitation radiation intensity of 0.25 W cm^{-2}.

an energy E = 16979.35 cm^{-1} is 3. In accordance with the selection rules for dipole transitions, $\Delta J = 0, \pm 1$; therefore, the number J for the second excited level with E = 33276.1 cm^{-1} should to be 2, 3, or 4. An attempt to find a transition to the state with E = 33726 cm^{-1} from the first excited state with E = 16757.039 cm^{-1} and J = 5, which corresponds to the first transition with λ_1 = 5967.641 Å and a large isotopic shift, was not successful. Therefore, the quantum number J of the second excited level with E = 33276.1 cm^{-1} is 2 or 3. Hence, transitions from the ground state to the first excited state with a moment J equal to 3 or 4 should be sought for.

Among the first transitions from the ground state to the levels with J = 3, there are two known transitions: with λ_1 = 5622.105 Å to the level E = 17786.93 cm^{-1} and with λ_1 = 6289.741 Å to the level E = 15898.91 cm^{-1}. The isotopic frequency shifts of these transitions are listed in Table 3. Transitions to the level with E = 33726.1 cm^{-1} were found for both upper levels; therefore, photoionisation may occur via the autoionising state with E = 50474 cm^{-1} (Fig. 3). The existence of a photoionisation scheme where the frequencies (wavelengths) of the second and third transitions do not coincide, allowed us to investigate the spectral profile of the absorption line on the autoionising transition between the levels with E = 33726.1 cm^{-1} and 50474 cm^{-1} (Fig. 4). It can be seen in Fig. 4 that the line profile is rather wide and has a fairly atypical structure.

Table 3. Isotopic frequency shifts for the first-stage transitions (in MHz).

Transition line wavelength/Å	$\Delta\nu_{142-144}$	$\Delta\nu_{144-146}$	$\Delta\nu_{146-148}$	$\Delta\nu_{148-150}$	References
6289.741	–674	–638	–670	–803	[14]
5622.105	+600 (30)	+615 (30)	+702 (40)	+1131 (40)	This study

We also investigated the dependences of the photoion current on the laser beam intensity for each transition; the results obtained for the first two stages of the schemes under consideration are listed in Table 4.

The dependence of the photoion current on the laser beam intensity for the third stage, obtained by tuning the third-

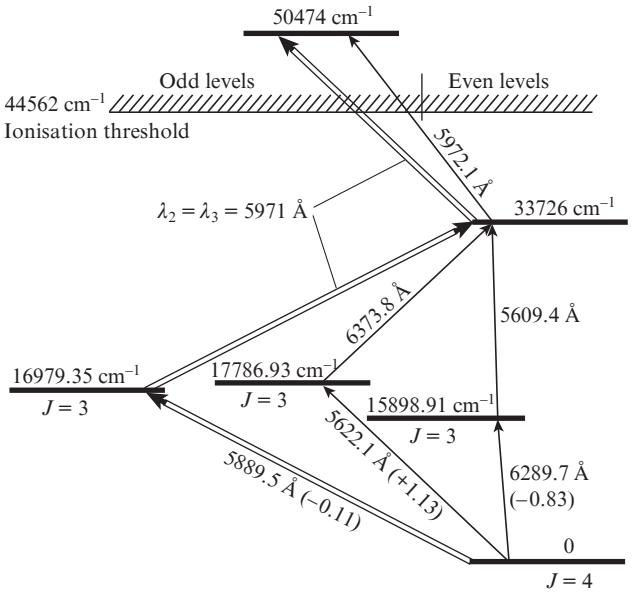

Figure 3. Nd I photoionisation schemes. Double lines show the photoionisation scheme proposed in [8]. The isotopic shifts (in GHz) between the frequencies of transitions in ^{148}Nd and ^{150}Nd are given in parentheses.

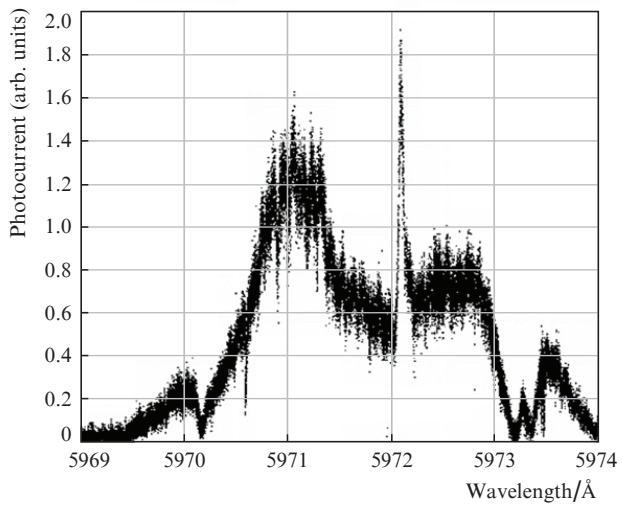

Figure 4. Spectral profile of the autoionising transition line between the levels with $E = 33726$ cm^{-1} and 50474 cm^{-1} (the FWHM of the peak at $\lambda = 5972.1$ Å is 4.7 GHz). Wavelength scanning was performed at an average radiation intensity of 0.12 W cm^{-2}.

Table 4. Transition saturation intensities for the first two excitation stages in Nd I photoionisation schemes.

Stage	Transition line wavelength/Å	Average saturation intensity/W cm^{-2}
First	6289.74	0.06
Second	5609.40	0.06
First	5622.10	< 0.015
Second	6273.84	4

stage radiation wavelength to the peak with $\lambda = 5972.1$ Å, is shown in Fig. 5. The saturation of the transition calls for an average intensity of 6 W cm^{-2}, which corresponds to a photo-

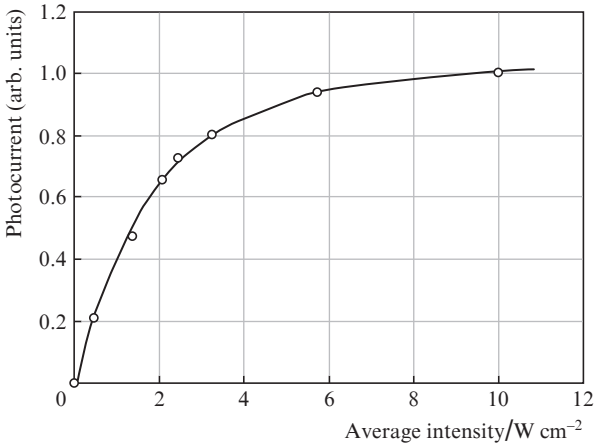

Figure 5. Dependence of the photoion current on the average laser beam intensity in the third stage in the scheme with $\lambda_1 = 6289.7$ Å, $\lambda_2 = 5609.4$ Å, and $\lambda_3 = 5972.1$ Å, at average radiation intensities in the first and second excitation stages of 0.18 and 0.15 W cm^{-2}, respectively.

ionisation cross section of $(5 \pm 1) \times 10^{-16}$ cm^2. The photoionisation scheme with $\lambda_1 = 6289.7$ Å, $\lambda_2 = 5609.4$ Å and $\lambda_3 = 5972.1$ Å corresponds to the problem stated, because the photoionisation cross section for the transition with $\lambda_3 = 5972.1$ Å is sufficiently large. At the same time, the isotopic frequency shift of the first transition ($\Delta\nu_{148-150} = -803$ MHz) exceeds the isotopic frequency shift of –110 MHz of the first transition with $\lambda_1 = 5889.5$ Å in the scheme considered in [8] by a factor of more than 7 and makes it possible to reach the desired photoionisation selectivity. Thus, the scheme found can be used in a laboratory setup for ^{150}Nd preparation. It is not reasonable to apply the scheme with $\lambda_1 = 5622.11$ Å, $\lambda_2 = 6273.84$ Å, and $\lambda_3 = 5972.1$ Å because of the high expenditures on the second-stage saturation.

3. Development of the laser system

The laser system of a technological AVLIS complex should provide highly efficient selective photoionisation of ^{177}Lu and ^{63}Ni radionuclides and ^{150}Nd isotope. A necessary condition for highly efficienct photoionisation is simultaneous saturation of each transition in the corresponding photoionisation scheme. Table 5 contains the wavelengths and average laser beam intensities corresponding to the saturation of transitions in the developed photoionisation schemes for lutetium, nickel, and neodymium atoms [3, 4].

Table 5. Wavelengths and average laser beam intensities corresponding to the saturation of transitions in the photoionisation schemes of neodymium, lutetium, and nickel atoms.

Stage	Element	Wavelength/Å	Intensity/W cm^{-2}
First	Nd	6289.74	0.06
	Lu	5404.16	0.01
	Ni	3222.58	0.08
Second	Nd	5609.40	0.06
	Lu	5350.59	0.01
	Ni	5464.01	0.02
Third	Nd	5972.1	6
	Lu	6180.06	2
	Ni	5442.16	5

Concerning the light power and spectral, frequency and spatial characteristics, a DL system pumped by a CVL can be considered efficient for the AVLIS process [15]. The CVL radiation has two components with approximately equal intensities at wavelengths of λ = 5106 and 5782 Å, due to which the spectral range of efficient DL generation is fairly wide. Recently, diode-pumped solid-state lasers with frequency doubling in a nonlinear crystal (λ = 5321 Å) have more often been used for DL pumping [16, 17]; these lasers are characterised by high energy efficiency and durability. However, having similar energy and temporal characteristics of radiation, the pump source used in this case significantly narrows the spectral range of efficient DL generation and, therefore, limits the possibilities of selective laser photoionisation.

The transition saturation conditions must be satisfied throughout the entire irradiation zone in the region of interaction with atomic vapour; therefore, an important factor is the laser-beam diameter. A decrease in the transverse beam size, on the one hand, imposes less stringent requirements on the output DL power and, on the other hand, increases the laser beam divergence and, therefore, reduces the length of the zone where the laser intensity can arbitrarily be considered constant.

When the laser beam diameter is less than 10 mm, it is rather difficult to converge several beams into one and transport them jointly to the separating complex. This condition determines the main energetic parameters of the laser system: the average laser power of the third stage should to be 2–6 W, depending on the type of selected isotope.

The laser complex consists of a set of wavelength-tunable pulsed DLs, pumped by a CVL system.

4. Pump laser

The CVL system is based on self-heating active elements (AEs) of the LT-40Cu 'Crystal' series (Research and Production Corporation 'Istok') [18] and thyratron modulators according to the master oscillator–amplifier scheme.

The CVL oscillator is based on the scheme of double-pass superluminescence amplification (Fig. 6). A special three-lens achromatic system (*1–3*) with a diaphragm (*4*) is used to 'purify' radiation spatially and form a weakly divergent beam with a diameter approximately equal to the AE channel diameter (20 mm).

The average output power of the CVL master oscillator is 2.5–3 W (radiation at λ = 5106 and 5782 Å, pulse repetition frequency 10 kHz, pulse duration 20–25 ns). The radiation of CVL master oscillator has an intensity profile close to Π-shaped (with homogeneity better than 90%), divergence of no more than 0.4 mrad, linear polarisation, and highly stable directional pattern (instability of no more than 0.05 mrad h^{-1}). These parameters of laser radiation promote its further successful amplification in the AE of the CVL amplifier, as well as efficient and stable conversion into the DL radiation. The output power of the CVL amplifier increases to 40–42 W without any significant deterioration of the spatial and polarisation characteristics of radiation. Temporal matching of CVL AEs is performed using an electron system [19] reducing the triggering time spread to ± 1 ns.

The ratio of the average powers of the green (λ = 5106 Å) and yellow (λ = 5782 Å) components of CVL radiation is ~5/4 (23 W/17 W). The components are spatially separated using a dichroic mirror [(*5*), Fig. 6], after which two pump beams are directed to the DL system.

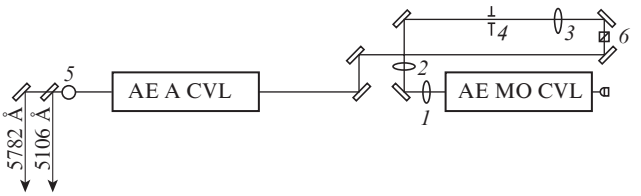

Figure 6. CVL optical scheme [master oscillator (MO)–amplifier (A)]: (*1–3*) three-lens achromatic system; (*4*) diaphragm; (*5*) dichroic mirror; (*6*) polarisation cube.

5. Dye lasers

The DL system (Fig. 7) contains three independent channels, designed according to the master oscillator–amplifier scheme. One of the DL channels is pumped by the yellow component of CVL radiation (λ = 5782 Å), and the two others are pumped by the green component (λ = 5106 Å). Depending on the photoionisation scheme in use (Table 5), one or two amplifiers are applied in the third-stage channels.

The DL master oscillators are constructed according to the Littman scheme [20] with one selecting element (diffraction grating operating in the grazing incidence regime) and radiation extraction into zero diffraction order. The output power of single-mode radiation is 150–200 mW (at a pump power of 1.5–2 W), the spectral linewidth (FWHM) is 100–130 MHz, the nonselective background component does not exceed 0.3%, and the pulse FWHM is 15–18 ns. The intensity distribution profile and beam divergence are close to Gaussian ($M^2 \approx 1.5$); more detailed information about the DL master oscillator can be found in [21].

The ionisation of ^{177}Lu, ^{63}Ni, and ^{150}Nd atoms in specific schemes (Table 5) is performed using the most efficient (from our point of view) laser dyes: PM556, PM567, PM597 (pumping with λ = 5106 Å) and SR640, Cresyl Violet (pumping with λ = 5782 Å). The experimental wavelength dependences of single-mode efficiency of the DL master oscillator for the aforementioned dyes are presented in Fig. 8.

The DL amplifiers operate in the longitudinal pump geometry [18, 22], which allows one to obtain high efficiency of pump radiation conversion and form output beams with a sufficiently uniform intensity profile [23]. The efficiency of the amplifiers in laser systems based on the chosen dyes is demonstrated in Fig. 9, which shows experimental dependences of the pump radiation conversion efficiency on gain.

To generate UV radiation (the first excitation stage for ^{63}Ni atoms; λ_1 = 3222.584 Å), the DL frequency is doubled in a nonlinear crystal [second-harmonic generation (SHG), Fig. 7]. The output radiation power at λ_1 = 3222.584 Å is ~0.3–0.35 W for a SHG efficiency of ~12%–15% (β-BBO crystal 4×4×5 mm in size, phase-matching angles θ = 39° and φ = 90°).

The radiation powers in all channels of the DL system and for all ionised elements are presented in Fig. 7. The maximum total average power of the three DL beams is 12 W (5 W + 1 W + 6 W), a value corresponding (at a pump power of 40 W) to a conversion efficiency of 30%. There are DL systems with efficiencies of 40%–50%; however, these values were obtained only due to the efficient operation of the final DL amplifiers at much higher pump powers [15]. It was possible to

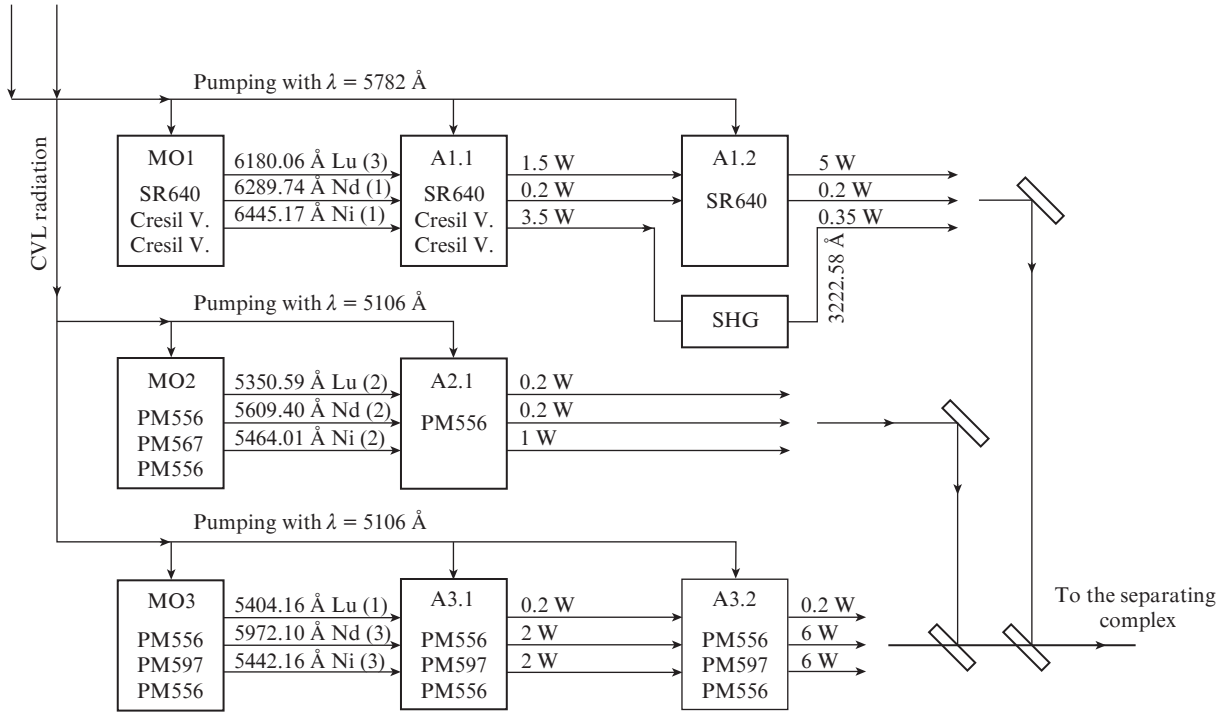

Figure 7. Block diagram of the DL system. The wavelengths and average output powers are indicated near each ray, and the ionisation stage numbers are given in parentheses. The laser dyes used for ionisation of a specific element are indicated for each MO and A; SHG is the second harmonic generator.

make the developed system highly efficient due to the use of the longitudinal pump geometry in DL amplifiers, choice of appropriate design of DL and CVL master oscillators, and the experimental choice of most efficient dyes.

The radiation beams at the amplifier output were telescoped to a transverse diameter of 10–12 mm; they were converged into one beam by semitransparent and/or dichroic mirrors. The radiation wavelength of each DL was monitored using precise LM007 wavelength meters (Laser 2000, GmbH), which provide an extremely high accuracy in wavelength measurements (with an error as low as ~0.0005 Å). These devices were also used as a stabilised reference when switching any DL into the regime of active wavelength stabilisation during ionisation. The DL lasing frequency was maintained automatically by controlling the length of the DL master oscillator cavity; the deviation of the lasing line centre from a specified value in the long-term stabilisation regime did not exceed ± 40 MHz.

To make it possible to switch the laser system to the spectral range of one of three ionisation schemes, the number of dye solution circulation systems was increased to 10 (according to the number of working dyes for the DL oscillators and

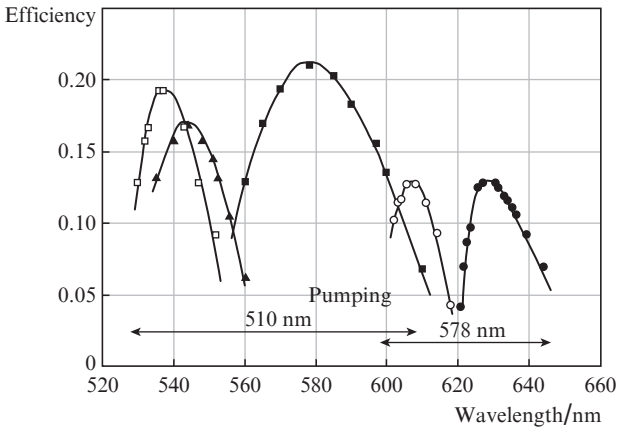

Figure 8. Dependences of the lasing efficiency on the wavelength of single-mode radiation from DL master oscillator (pumped by CVL) for laser dyes (□) PM556 in ethanol–distilled water (10/1) mixture, (▲) PM567 in ethanol, (■) PM597 in *n*-heptane, (○) SR640 in ethanol–distilled water (2/1), and (●) Cresyl Violet in ethanol. All the dyes are produced by Exciton (United States).

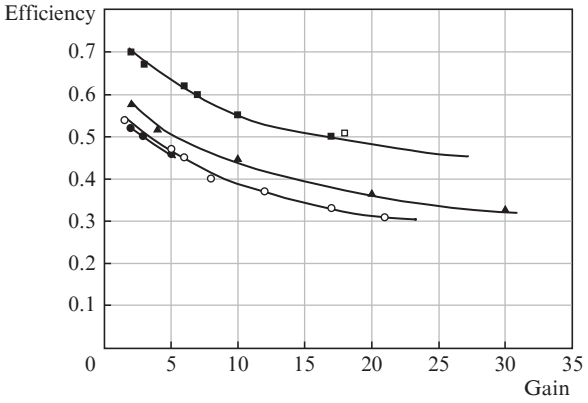

Figure 9. Dependences of the efficiency of DL amplifiers (with longitudinal pumping by CVL radiation) on gain for the following dyes (the measurement wavelengths are indicated in parentheses): (□) PM556 (λ = 540 nm), (▲) PM567 (λ = 550 nm), (■) PM597 (λ = 580 nm), (○) SR640 (λ = 606 nm), and (●) Cresyl Violet (λ = 635 nm).

amplifiers). The replacement of dye in any element of the DL system implies reconnection of input and output hose pipes of laser cells from one pumped system to another (without applying the drain/filling procedures, careful washing of the system, replacement of filter elements, etc.). As practice showed, small amounts ($\sim$1 cm^3) of dye solution residue on the internal walls of cells and hose pipes do not affect the lasing characteristics of the new solution with a volume of $\sim$10 L.

Concerning the optical elements, to switch the laser system to another scheme, one should replace dichroic mirrors for beam convergence and rearrange the rotational mirror unit of the master oscillator cavity into the angular position corresponding to the lasing spectrum. Since most of the optical elements of the system (mirrors, splitters, window cells, etc.) have broadband (530–600 nm, 600–650 nm) dielectric (both reflection and antireflection) coatings, it is not necessary to replace them. The above-mentioned technical solutions made it possible to rearrange the laser system for a specific element during one working day.

6. Conclusions

Photoionisation schemes characterised by similar isotopic shifts and effective photoionisation cross sections were found for an important practical application: separation of lutetium, nickel, and neodymium isotopes. This advance made it possible to consider the possibility of forming a laser complex for laboratory production of ^{177}Lu and ^{63}Ni radionuclides and ^{150}Nd isotope using a compact and mobile laser system based on CVL-pumped DLs.

The developed laser system made it possible to convert for the first time the CVL pump radiation into high-quality (single-mode, wavelength-stabilised in the range of 535–645 nm, with a divergence close to the diffraction one) radiation of three DLs with a 30% efficiency at a low average power of pump radiation (20–40 W).

The pump laser is based on only two LT-40Cu Crystal AEs, due to which the laser system maintenance can be supported at the grant level.

Acknowledgements. This work was supported by the Russian Science Foundation (Project No. 17-13-01180).

References

1. Kudrin L.P., Novikov V.M., Blinkin V.L. *Metody razdeleniya izotopov, osnovannye na selektivnom fotovozbuzhdenii (Otchet IAE-1986); Broshyura RNTs 'Kurchatovskii institut'* (Methods for Separating Isotopes Based on Selective Photoexcitation (Report IAE-1986); Booklet of NRC 'Kurchatov Institute' (Moscow: 2002) p. 39.
2. Letokhov V.S. *O vozmozhnosti razdeleniya izotopov metodami rezonansnoi fotoionizatsii atomov i fotodissotsiatsii molekul lazernym izlucheniem (Otchet FIAN, 1969); Preprint ISAN SSSR No. 1* [On the Possibility of Separating Isotopes by Methods of Resonance Photoionisation of Atoms and Photodissociation of Molecules Using Laser Radiation (FIAN Report, 1969)]; Preprint ISAN USSR No. 1 (Moscow, 1979) p. 1.
3. D'yachkov A.B., Firsov V.A., Gorkunov A.A., Labozin A.V., Mironov S.M., Panchenko V.Y., Semenov A.N., Shatalova G.G., Tsvetkov G.O. *Appl. Phys. B*, **121**, 425 (2015).
4. Tsvetkov G.O., D'yachkov A.B., Gorkunov A.A., Labozin A.V., Mironov S.M., Firsov V.A., Panchenko V.Ya. *Quantum Electron.*, **47** (1), 48 (2017) [*Kvantovaya Elektron.*, **47** (1), 48 (2017)].
5. Babichev A.P., Grigor'ev I.S., Grigor'ev A.I., Dorovskii A.P., D'yachkov A.B., Kovalevich S.K., Kochetov V.A., Kuznetsov V.A., Labozin V.P., Matrakhov A.V., Mironov S.M., Nikulin S.A., Pesnya A.V., Timofeev N.I., Firsov V.A., Tsvetkov G.O., Shatalova G.G. *Quantum Electron.*, **35** (10), 879 (2005) [*Kvantovaya Elektron.*, **35** (10), 879 (2005)].
6. Balysh A.Y., Labozin V.P., Semenov S.V. *Nucl. Phys. B: Proc. Suppl.*, **237-238**, 7 (2013).
7. https://web.archive.org/web/20080821193614/http://www.usec.com/NewsRoom/NewsReleases/USECInc/1999/1999-06-09-USEC-Inc-Suspends-AVLIS.htm.
8. Zyuzikov A.A., Mishin V.I., Fedoseev V.N. *Opt. Spektrosk.*, **64** (3), 480 (1988).
9. Martin W.C., Zalubas R., Hagan L. *Atomic Energy Levels. The Rare-Earths Elements* (Washington: NBS (US), 1978) p. 124.
10. King A.S. *Astrophys. J.*, **78** (1), 9 (1933).
11. Biémont E., Quinet P., Svanberg S., Xu H.L. *J. Phys. B: At. Mol. Opt. Phys.*, **37**, 1381 (2004).
12. Smirnov Yu.M. *Teplofiz. Vys. Temp.*, **41** (2), 211 (2003).
13. Ahmad S.A., Saskena G.D. *Spectrochimica Acta*, *Part B*, **35**, 81 (1980).
14. Van Leeuwen K.A.H., Eliel E.R., Post B.H., Hogervorst W. *Z. Phys. A: At. Nucl.*, **301**, 95 (1981).
15. Bass I.L., Bonanno R.E., Hackel R.P., et al. *Appl. Opt.*, **31**, 6993 (1992).
16. Hyunmin Park, Duck-Hee Kwon, Yongho Cha, Sungmo Nam, Tak-Soo Kim, Jaemin Han, Yongjoo Rhee, Do-Young Jeong, Cheol-Jung Kim. *J. Korean Phys. Soc.*, **49** (1), 382 (2006).
17. Mishra G.K. *RRCAT Newsletter*, **29** (2), 15 (2016).
18. Lyabin N.A., Chursin A.D., Ugol'nikov S.A., Koroleva M.E., Kazaryan M.A. *Quantum Electron.*, **31** (3), 191 (2001) [*Kvantovaya Elektron.*, **31** (3), 191 (2001)].
19. Firsov V.A., Suslov V.I., Belousov A.B., et al. *Sb. dokl. VI Vseros. (mezhdunar.) nauchnoi konf. 'Fiziko-khimicheskie protsessy pri selektsii atomov i molekul'* (Proc. VI All-Russia (Int.) Sci. Conf. 'Physical and Chemical Processes in Selection of Atoms and Molecules') (Zvenigorod: TsNIIatom-inform, 2002) p. 235.
20. Littman M.G. *Appl. Opt.*, **23**, 4465 (1984).
21. Grigoriev I., Diachkov A., Kuznetzov V., Labosin V., Firsov V. *Proc. SPIE Int. Soc. Opt. Eng.*, **5121**, 411 (2003).
22. D'yachkov A.B., Labozin V.P. *Sb. dokl. VI Vseros. (mezhdunar.) nauchnoi konf. 'Fiziko-khimicheskie protsessy pri selektsii atomov i molekul'* (Proc. VI All-Russia (Int.) Sci. Conf. 'Physical and Chemical Processes in Selection of Atoms and Molecules') (Zvenigorod: TsNIIatom-inform, 2001) p. 132.
23. Grigor'ev I.S., D'yachkov A.B., Labozin V.P., et al. *Quantum Electron.*, **34** (5), 447 (2004) [*Kvantovaya Elektron.*, **34** (5), 447 (2004)].